

# Entropy production in hot-phonon energy conversion to electric potential

Seungha Shin and Massoud Kaviany<sup>a)</sup>

Department of Mechanical Engineering, University of Michigan, Ann Arbor, Michigan 48109, USA

(Received 18 June 2013; accepted 8 August 2013; published online 27 August 2013)

We apply phonon and electron nonequilibrium-population statistical entropy analysis to the recently introduced phonon energy to electric potential conversion heterobarrier with its height optimized for optical phonon absorption under steady electric current. The entropy production rates for phonon and electron subsystems depend on their interaction kinetics and occupancy distributions, indicating the direction of the processes. Under upstream thermal equilibrium among electrons and acoustic and optical phonons, we predict an upper limit of 42% energy conversion for GaAs heterobarrier at 300 K, while the reported Monte Carlo prediction of 19% efficiency is below this limit. We show that for upstream electrons in thermal equilibrium with the acoustic phonons, while under supply of hot optical phonons, the conversion efficiency increases significantly, making integration of the barrier into optical phonon emitting circuits and devices very attractive. © 2013 AIP Publishing LLC. [<http://dx.doi.org/10.1063/1.4819217>]

## I. INTRODUCTION

In any energy conversion processes, the final states correspond to the maximum system entropy, and the system entropy increase is accompanied by decrease in the availability of these systems to do work.<sup>1,2</sup> In the limit of reversible interaction, there is no net entropy increase, and the maximum energy conversion efficiency is achieved, i.e., the Carnot efficiency, which is determined from the equilibrium temperatures and heat flow rate.<sup>1-3</sup> Thus, tracking the system entropy, the energy conversion system can be verified and the upper limit of its conversion efficiency is theoretically predicted. For example, the entropy production in the anti-Stokes laser cooling has been originally analyzed in Ref. 4 and recently in Ref. 5, showing that the laser cooling does not violate the thermodynamic laws and predicting the maximum cooling performance. Thermoelectric energy conversion is also studied with the theoretical description of the coupled thermodynamic forces and fluxes.<sup>6,7</sup>

In this research, through the entropy analysis of energy carriers, we study various energy conversions between electron ( $e$ ) and phonon ( $p$ ) subsystems, and in particular the recently reported phonon recycling using a heterobarrier<sup>8</sup> is analyzed. As shown in Fig. 1, the barrier structure converts the phonon energy (or flux  $q_p$ ) to electron thermal ( $q_e$ ) and potential energy ( $p_e$ ) through a phonon absorption favorable condition and barrier transition. The barrier with a height ( $\phi_b$ ) nearly equal to the optical phonon energy ( $E_{p,O} = \hbar\omega_{p,O}$ , where  $\hbar$  is the reduced Planck constant, and  $\omega_{p,O}$  is the angular frequency of singly presented optical phonon) can effectively absorb the overpopulated nonequilibrium (i.e., hot) phonons, since the structure creates large population of the low energy electrons. A large internal electric field ( $e_e$ ) is introduced downstream of the barrier to maintain the electric current density ( $j_e$ ), and through this structure, an electric potential power gain ( $\Delta p_e = \Delta\phi_e j_e$ , where  $\phi_e$  is electrochemical potential gain) can

be expected. Here, the electron energy distributions are under nonequilibrium due to the barrier, thus the entropy for this nonequilibrium should be addressed. However, the entropy and temperature are the conjugate property pair,<sup>3</sup> so in the classical thermodynamic treatment it is a challenge to define the entropy under nonequilibrium properties, since it requires a corresponding definition of the nonequilibrium temperatures. This can be overcome by using the statistical entropy of microstates under nonequilibrium conditions, so we study the statistical entropy production to predict the theoretical upper limit of phonon-electron energy conversion.

## II. ENTROPY ANALYSES

In the Boltzmann formulation,<sup>9</sup> the statistical entropy is  $S = k_B \ln W$ , where  $k_B$  is the Boltzmann constant and  $W$  is the number of microstates for a given macrostate. Considering the properties of principal energy carriers, the statistical entropies for phonon and electron are<sup>10-12</sup>

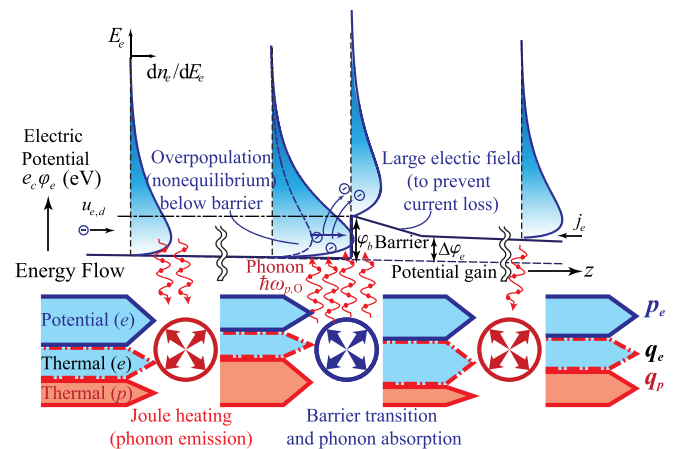


FIG. 1. Schematic of the phonon-electron energy conversion processes in the barrier transition. Since the barrier does not allow for the transmission of electrons with energy lower than the potential barrier, the electrons which are also favorable to phonon absorption become more populated. To maintain the electric current, a large internal electric field is needed downstream of the barrier.

<sup>a)</sup>Electronic mail: kaviany@umich.edu

$$S_p = \int_0^\infty k_B D_p [(f_p + 1) \ln(f_p + 1) - f_p \ln f_p] dE_p, \quad (1)$$

$$S_e = - \int_{-\infty}^\infty k_B D_e [(1 - f_e) \ln(1 - f_e) + f_e \ln f_e] dE_e. \quad (2)$$

Here  $D_i$  is the density of states [per unit volume (or a primitive cell) and per unit energy range] and  $f_i$  is the occupancy function, and both  $D_i$  and  $f_i$  depend on carrier energy  $E_i$  ( $i = e$  or  $p$ ). From the occupancy functions (Bose-Einstein  $f_p$  for phonon and Fermi-Dirac  $f_e$  for electron), the temperatures at energy level  $E_p$  or  $E_e$  are [using the Fermi level  $E_F$  as the chemical potential  $\mu_c$  (Ref. 13)]

$$T_p(f_p, E_p) = \frac{E_p}{k_B [\ln(f_p + 1) - \ln f_p]}, \quad \text{and} \quad (3)$$

$$T_e(f_e, E_e) = \frac{E_e - E_F}{k_B [\ln(1 - f_e) - \ln f_e]}.$$

### A. Interactions between phonon subsystems

Electrons in many polar semiconductors (e.g., GaAs, GaN, and SiC) are dominantly scattered by the longitudinal optical (LO) phonons, and due to the low momentum and smaller decay rate, the LO phonon mode can be overpopulated during the energy conversion processes.<sup>14,15</sup> These overpopulated hot phonons decay through the downconversion to acoustic phonon modes (three-phonon process) with a decay rate  $\dot{\gamma}_{p-p,down}$  (which can be calculated using the Fermi golden rule<sup>8,16</sup>) until the equilibrium occupancy is reached. The entropy change through the interactions between the phonon subsystems (LO and other phonon modes) during the hot LO phonon relaxation is addressed below, and a non-dispersed, single-phonon energy approximation ( $E_{p,LO} = \hbar\omega_{p,LO}$ ) is employed for the LO phonons. In a primitive cell with two atoms,  $\int_0^\infty D_{p,LO} dE_{p,LO} = 1$  (where  $D_{p,LO}$  is the density of states per a primitive cell per unit energy range), and the energy ( $\langle \rangle$  indicates the subsystem ensemble average) and entropy of the LO phonon mode are

$$\langle E_{p,LO} \rangle = f_{p,LO} E_{p,LO},$$

$$S_{p,LO}(T_{p,LO}) = k_B [(f_{p,LO} + 1) \ln(f_{p,LO} + 1) - f_{p,LO} \ln f_{p,LO}]. \quad (4)$$

Through the relaxation, the energy and entropy of each subsystem change, and the change rates for the phonon subsystem with LO mode are

$$\frac{d\langle E_{p,LO} \rangle}{dt} = \frac{df_{p,LO}}{dt} E_{p,LO}, \quad \text{and} \quad \frac{dS_{p,LO}}{dt} = k_B \frac{df_{p,LO}}{dt} \ln \left( \frac{f_{p,LO} + 1}{f_{p,LO}} \right). \quad (5)$$

Using the relaxation time approximation ( $df_{p,LO}/dt = -\dot{\gamma}_{p-p,down} f_{p,LO}$ ),<sup>17</sup> the rate of energy change in a primitive cell is

$$\frac{d\langle E_{p,LO} \rangle}{dt} = -\dot{\gamma}_{p-p,down} f_{p,LO} E_{p,LO} (= -\dot{\gamma}_{p-p,down} \langle E_{p,LO} \rangle). \quad (6)$$

With the phonon temperature defined in Eq. (3), the entropy change is found as

$$\frac{dS_{p,LO}}{dt} = \frac{1}{T_{p,LO}} \frac{d\langle E_{p,LO} \rangle}{dt} = -\frac{\dot{\gamma}_{p-p,down} \langle E_{p,LO} \rangle}{T_{p,LO}}. \quad (7)$$

Assuming that the other phonon modes ( $p, A$ ) are in equilibrium (because of faster relaxation rate among them), only the nonequilibrium between LO and A phonon modes is considered. Without any external source, the total phonon system energy is conserved ( $dE_p/dt = dE_{p,LO}/dt + dE_{p,A}/dt = 0$ ). Then from Eq. (6), we have

$$\frac{d\langle E_{p,A} \rangle}{dt} = -\frac{d\langle E_{p,LO} \rangle}{dt} = \dot{\gamma}_{p-p,down} f_{p,LO} E_{p,LO}, \quad (8)$$

where the total phonon energy with mode A in a primitive cell,  $\langle E_{p,A} \rangle = \int D_{p,A} f_{p,A} E_p dE_p$ . The entropy production rate is

$$\frac{dS_{p,A}}{dt} = \int k_B D_{p,A} \frac{df_{p,A}}{dt} \ln \left( \frac{f_{p,A} + 1}{f_{p,A}} \right) dE_p$$

$$= \int D_{p,A} \frac{df_{p,A}}{dt} \frac{E_p}{T'_{p,A}(E_p)} dE_p, \quad (9)$$

where  $T'_{p,A}$  is the temperature of energy level  $E_p$  (Ref. 18) in Eq. (3). With an equilibrium temperature [ $T_{p,A} = T'_{p,A}(E_p)$ ], the total phonon entropy production rate is

$$\frac{dS_p}{dt} = \frac{dS_{p,A}}{dt} + \frac{dS_{p,LO}}{dt} = \frac{1}{T_{p,A}} \frac{d\langle E_{p,A} \rangle}{dt} + \frac{1}{T_{p,LO}} \frac{d\langle E_{p,LO} \rangle}{dt}$$

$$= \left( \frac{1}{T_{p,LO}} - \frac{1}{T_{p,A}} \right) \frac{d\langle E_{p,LO} \rangle}{dt}$$

$$= \left( \frac{1}{T_{p,A}} - \frac{1}{T_{p,LO}} \right) \dot{\gamma}_{p-p,down} \langle E_{p,LO} \rangle. \quad (10)$$

In the presence of hot LO phonons ( $T_{p,LO} > T_{p,A}$ ), the total entropy increases, and the rate of entropy increase is higher under a more pronounced nonequilibrium phonons (larger temperature difference between LO phonon and other phonon modes).

### B. Electron-phonon interactions

The energy and entropy changes in the electron-phonon ( $e-p$ ) interactions are determined based on their kinetics. Simplifying the interaction system (as a system with the electron-LO phonon interaction only available), the rates of the LO phonon energy and entropy changes are (in phonon emission, energy is converted from electron to phonon, increasing  $f_{p,LO}$ )

$$\frac{d\langle E_{p,LO} \rangle}{dt} = \int (\dot{\gamma}_{e \rightarrow p} - \dot{\gamma}_{p \rightarrow e}) f_e D_e E_{p,LO} dE_e, \quad (11)$$

$$\frac{dS_{p,LO}}{dt} = \frac{1}{T_{p,LO}} \frac{d\langle E_{p,LO} \rangle}{dt} = \frac{E_{p,LO}}{T_{p,LO}} \int (\dot{\gamma}_{e \rightarrow p} - \dot{\gamma}_{p \rightarrow e}) f_e D_e E_{p,LO} dE_e, \quad (12)$$

where  $\dot{\gamma}_{p \rightarrow e}$  and  $\dot{\gamma}_{e \rightarrow p}$  are the phonon absorption and emission rates. Using the energy conservation and the total electron thermal energy  $\langle E_e \rangle = \int (E_e - E_F) D_e f_e dE_e$ , the electron energy change becomes

$$\frac{d\langle E_e \rangle}{dt} = \int (E_e - E_F) D_e \frac{df_e}{dt} dE_e = -\frac{d\langle E_{p,LO} \rangle}{dt}. \quad (13)$$

The electron entropy production rate is obtained from the time derivative of Eq. (2), and using the definition of the electron temperature in Eq. (3) it can be written as

$$\frac{dS_e}{dt} = \int_{-\infty}^{\infty} k_B D_e \frac{df_e}{dt} \ln \left( \frac{1-f_e}{f_e} \right) dE_e = \int_{-\infty}^{\infty} D_e \frac{df_e}{dt} \frac{E_e - E_F}{T_e(E_e)} dE_e. \quad (14)$$

If the electrons are in equilibrium,  $T_e$  is constant over all energy levels [ $T_e = T_e(E_e)$ ] and  $dS_e/dt$  becomes simply  $(1/T_e)d\langle E_e \rangle/dt$ . Then, the total entropy production rate in the  $e$ - $p$  interaction system is given as

$$\frac{dS_{p,LO}}{dt} + \frac{dS_e}{dt} = \left( \frac{1}{T_{p,LO}} - \frac{1}{T_e} \right) \frac{d\langle E_{p,LO} \rangle}{dt} \geq 0. \quad (15)$$

As expected, when the heat flows from higher to lower temperature subsystem, the entropy always increases, and the entropy increase originates from the nonequilibrium between the subsystems.

### C. Steady electrical current

The barrier energy conversion system is applied to a system with a steady electric current, and the thermodynamic analysis of the system is discussed in this subsection. In the wavevector ( $\kappa_e$ ) space, the electron distribution without an average drift is symmetric in equilibrium. With a parabolic band structure in  $\Gamma$ -valley, the electron kinetic energy ( $E_{e,k}$ ) is proportional to the square of the distance from the origin in the  $\kappa$ -space ( $E_{e,k} = \hbar^2 |\kappa_e|^2 / 2m_{e,e}$ , where  $m_{e,e}$  is the electron effective mass).<sup>19</sup>

In the presence of an electric field ( $e_e$ ), the electrons accelerate and gain momentum in the applied field direction. As Fig. 2 shows, considering a fixed  $e_e$  only in the  $z$  direction ( $e_e = e_{e,z}z$ ,  $z$  is a unit vector in the  $z$  direction), the electric potential drop over  $\Delta z$  is  $\Delta\varphi_e = e_{e,z}\Delta z$ , and this potential drop leads to a kinetic energy or momentum gain, which corresponds to the momentum change  $[\hbar\Delta\kappa_e$ , where  $\Delta\kappa_e = (2m_{e,e}\Delta\varphi_e)^{1/2}/\hbar$ ]. As a result, the electron distribution shifts, and the electron distribution changes to nonequilibrium. Since the electrons are scattered by various mechanisms and the higher-energy electrons (larger distance from the origin) have larger phonon emission rate than absorption (whereas low-energy electrons are phonon absorption favorable), the electron distribution has a finite bias in the  $\kappa$ -space ( $\kappa_{e,d}$ ), showing an average drift velocity ( $u_{e,d} = \hbar\kappa_{e,d}/m_{e,e}$ ). With a low electric field ( $e_e$ ), the electron drift is linearly proportional to the field, ( $u_{e,d} = \mu_e e_e$ ) and here the ratio of  $u_{e,d}$  and  $e_e$  is the electron mobility ( $\mu_e$ ).

For electrons in the  $\Gamma$ -valley of the lowest conduction band ( $0 < E_{e,k} < 0.29$  eV) in GaAs, using the parabolic

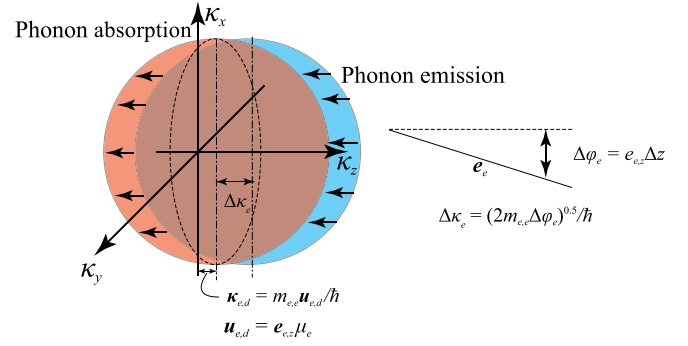


FIG. 2. The shift in the electron distribution in the  $\kappa$ -space caused by an electric field. Electrons with higher energy (larger distance from the origin in the  $\kappa$ -space) are favored for phonon emission, while the lower energy electrons are phonon-absorption favored. Due to the electron scattering (including the phonon absorption and emission), the electron distribution has a finite bias showing the electron drift velocity, and the bias is not significant compared to the average electron energy.

band assumption and  $m_{e,e} = 0.063m_e$  ( $m_e$  is free electron mass),<sup>20</sup> a drift velocity ( $u_{e,d}$ ) of  $2.3 \times 10^4$  m/s results in only 0.1 meV bias. [Even with a saturation velocity  $1.2 \times 10^5$  m/s (Ref. 21), the bias is only 2.5 meV.] Therefore, the bias caused by the electric current does not have a large effect on the distribution, and a symmetric and equilibrium distribution can be assumed in a simple electron drift.

Each particle contains the electrochemical potential ( $\varphi_e$ ), which is composed of a chemical potential ( $\mu_e$ , or Fermi level  $E_F$ ) and an electrostatic component ( $e_c V$ ,  $e_c$ : the electron charge and  $V$ : the electrostatic potential).<sup>7</sup> The change in the local Fermi level is generally referred to as the change in the electrochemical potential in the analysis of steady electric circuit ( $\Delta\varphi_e = \Delta E_F$ ). Including this chemical potential, the total electron energy is  $\langle E_e \rangle + E_F n_e$ , where  $n_e$  is the number (density or in a primitive cell) of electrons ( $= \int D_e f_e dE_e$ ) and  $\langle E_e \rangle$  is the sum of the electrostatic potential ( $\langle E_{e,p} \rangle$ ) and the electron kinetic energy ( $\langle E_{e,k} \rangle$ ). (In semiconductors, the electrostatic potential is  $E_{e,p} = E_c - E_F$  and the electron kinetic energy is  $E_{e,k} = E_e - E_c$ , where  $E_c$  is the conduction band edge.<sup>17</sup>)

Figure 3 describes the energy ( $j_E$ , W/m<sup>2</sup>) and entropy fluxes ( $j_S$ , W/m<sup>2</sup>-K) for steady, electric current. Here we consider a 1-D transport in the  $z$  direction (the properties in the lateral directions are assumed uniform, so the lateral transport is ignored) in a control volume which has boundaries  $L(z=0)$  and  $R(z=\Delta z)$ . Under steady-state condition ( $\partial E/\partial t = 0$ , no internal energy change), the total energy generation in a system is equivalent to the volume integral of the divergence of energy flux  $j_E$  and is zero (by energy conservation). Using the Gauss divergence theorem (and the surface normal unit vector  $s_A$ ), this becomes

$$\frac{dE}{dt} = \int_V \nabla \cdot j_E dV = \int_A j_E \cdot s_A dA = 0. \quad (16)$$

Here, the energy flux can be decomposed as

$$j_E = q_p + q_e + p_e (= q_p + q_e + E_F j_{n,e}), \quad (17)$$

where  $q_p$  and  $q_e$  are the phonon and electron thermal energy flux (heat flux) vectors, respectively, and  $E_F j_{n,e}$  (or  $p_e$ ) is the

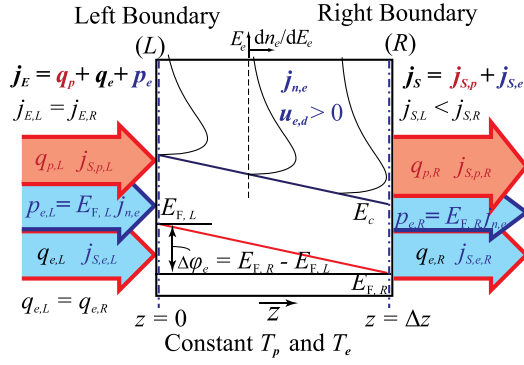


FIG. 3. The balance of energy flux ( $j_E$ ) and the entropy flux ( $j_S$ ) under 1-D steady electric current, with the arrow thickness representing the magnitude of energy flux. The system energy flux is constant ( $j_{E,L} = j_{E,R}$ ), while the system entropy increases through the control volume ( $j_{S,L} < j_{S,R}$ ). With constant temperatures (i.e., constant electron and phonon occupancies), the electrochemical potential is converted to phonon energy, and this results in the entropy production.

chemical energy flux.  $j_{n,e}$  ( $\text{m}^{-2}\text{s}^{-1}$ ) is the electron number flux given as

$$j_{n,e} = \int u'_{e,d} D_e f_e dE_e, \quad (18)$$

where  $u'_{e,d}$  is the drift velocity at  $E_e$ , and the electric current density is  $j_e = -e j_{n,e}$ . From Eq. (16), the net energy flux in 1-D transport system is

$$\int_A j_E \cdot s_A dA = A_z (j_{E,R} - j_{E,L}) = 0, \quad (19)$$

where  $A_z$  is the area normal to the transport direction  $z$ , and  $j_{E,R(\text{or}L)}$  is the  $z$ -direction component of energy flux at the right ( $R$ ) [or left ( $L$ )] boundary. This shows that only the energy fluxes at the left and right boundaries are required for the energy conservation. The total energy flux should be conserved ( $j_{E,z} = j_{E,R} = j_{E,L}$ ), but each component in  $j_E$  [Eq. (17)] varies because of interactions.

The phonon absorption and emission by  $e$ - $p$  interactions change the phonon energy flux in the  $z$  direction, so the net phonon emission in the control volume is

$$\Delta q_{p,z} = q_{p,R} - q_{p,L} = -\dot{S}_{p \rightarrow e} / A_z = -\int_0^{\Delta z} \dot{s}_{p \rightarrow e} dz, \quad (20)$$

where  $\dot{S}_{p \rightarrow e}$  is the phonon energy absorption rate (W) and  $\dot{s}_{p \rightarrow e}$  is the volumetric phonon absorption rate ( $\text{W}/\text{m}^3$ ). [When only the LO phonon scattering is included,  $\dot{s}_{p \rightarrow e} = \int (\dot{\gamma}_{p \rightarrow e} - \dot{\gamma}_{e \rightarrow p}) E_{p,LO} f_e D_e dE_e$ , similar to Eq. (11).] The change in electron heat flux (in the  $z$  direction) is

$$\Delta q_{e,z} = q_{e,R} - q_{e,L} = \int (q'_{e,R} - q'_{e,L}) dE_e. \quad (21)$$

Here  $q'_{e,R(\text{or}L)}$  is the heat flux contribution of the electrons with  $E_e$  at the right (or left) boundary, i.e.,  $q'_{e,R(\text{or}L)}$

$= u'_{e,d,R(\text{or}L)} [E_e - E_{F,R(\text{or}L})] D_{e,R(\text{or}L)} f_{e,R(\text{or}L)}$ . From the particle number conservation,  $j_{n,e,z}$  is constant, i.e.,

$$\Delta j_{n,e,z} = j_{n,e,R} - j_{n,e,L} = \int (u'_{e,d,R} D_e f_{e,R} - u'_{e,d,L} D_e f_{e,L}) dE_e = 0, \quad (22)$$

and with the electrochemical potential gain  $\Delta \phi_e (= E_{F,R} - E_{F,L})$ , the change in the electrochemical potential flux ( $\Delta p_{e,z}$ ) in the  $z$  direction is

$$\Delta p_{e,z} = \Delta \phi_e j_{n,e,z} = (E_{F,R} - E_{F,L}) j_{n,e,z}. \quad (23)$$

Using Eqs. (20), (21), and (23) with the energy conservation,

$$\int_A j_E \cdot s_A dA = \Delta q_{p,z} + \Delta q_{e,z} + \Delta p_{e,z} = 0 \quad (24)$$

$$-\dot{S}_{p \rightarrow e} / A_z + \int (q'_{e,R} - q'_{e,L}) dE_e + \Delta \phi_e j_{n,e,z} = 0.$$

The entropy production rate under steady state is equal to the net entropy flux ( $\Delta j_{S,z}$ ) as in energy flux. The net electron entropy flux is

$$\Delta j_{S,e,z} = j_{S,e,R} - j_{S,e,L}, \quad (25)$$

and using the local statistical entropy  $S_e$  [Eq. (2)], the entropy flux ( $j_{S,e,z}$ ) in  $z$  direction is given as

$$j_{S,e,z} = \int S'_e u'_{e,d,z} dE_e$$

$$= - \int k_B D_e [(1 - f_e) \ln(1 - f_e) + f_e \ln(f_e)] u'_{e,d,z} dE_e. \quad (26)$$

With a low electron occupancy in semiconductor [ $\ln(1 - f_e) \approx -f_e$ ], the net electron entropy flux or entropy generation in the control volume becomes

$$\Delta j_{S,e,z} = \int (S'_{e,R} u'_{e,d,R} - S'_{e,L} u'_{e,d,L}) dE_e = \int \left( \frac{q'_{e,R}}{T'_{e,R}} - \frac{q'_{e,L}}{T'_{e,L}} \right) dE_e, \quad (27)$$

where  $q'_{e,R(\text{or}L)}$  and  $T'_{e,R(\text{or}L)}$  are the  $E_e$ -dependent heat flux contribution and temperature at the boundary  $R$  (or  $L$ ), and if the electrons are in equilibrium on both boundaries, this becomes

$$\Delta j_{S,e,z} = \frac{q_{e,R}}{T_{e,R}} - \frac{q_{e,L}}{T_{e,L}}. \quad (28)$$

The net phonon entropy flux or phonon entropy production rate is

$$\Delta j_{S,p,z} = \frac{dS_p}{dt} = \frac{1}{T_p} \frac{d\langle E_p \rangle}{dt} = -\frac{\dot{S}_{p \rightarrow e} / A_z}{T_p} = -\frac{\Delta q_{p,z}}{T_p}, \quad (29)$$

and using the energy conservation in Eq. (24), this can be written as

$$\Delta j_{S,p,z} = - \frac{\int (q'_{e,R} - q'_{e,L}) dE_e + \Delta \varphi_e j_{n,e,z}}{T_p}. \quad (30)$$

According to the second law of thermodynamics, the total entropy production rate should not be smaller than 0, i.e.,

$$\begin{aligned} \Delta j_{S,e,z} + \Delta j_{S,p,z} &\geq 0 \\ \int (S'_{e,R} u'_{e,d,R} - S'_{e,L} u'_{e,d,L}) dE_e & \\ \int \frac{(q'_{e,R} - q'_{e,L}) dE_e + \Delta \varphi_e j_{n,e,z}}{T_p} &\geq 0. \end{aligned} \quad (31)$$

Without scattering (friction), the conversion between the electron kinetic and potential energies ( $E_{e,k}$  and  $E_{e,p}$ ) will be reversible as in the mechanical system. However, as a result of the electron-phonon interactions or other scattering mechanisms (e.g.,  $e-e$ ), the electron system has a constant drift velocity in spite of the loss of electrochemical potential. Assuming the constant electron and phonon occupancy distributions, the temperatures on both boundaries are the same, and the electron heat flux ( $q_e$ ) is consistent [i.e.,  $D_e f_e$  for ( $E_e - E_F$ ) does not change]. Thus, the net phonon flux  $\Delta q_{p,z}$  is  $-\Delta \varphi_e j_{n,e,z}$  (according to the energy conservation, Eq. (24)], which is the known Joule heating  $\dot{S}_{e,J}$ . The total entropy production rate ( $\Delta j_{S,e,z} + \Delta j_{S,p,z}$ ) becomes  $-\Delta \varphi_e j_{n,e,z} / T = \dot{S}_{e,J} / T$ , and this shows that the entropy in the electric currents always increases, because of the voltage drop ( $\Delta \varphi_e < 0$ ) and electron drift ( $j_{n,e,z} > 0$ ).

### III. ENTROPY IN ENERGY CONVERSION SYSTEMS

In this section, using the analysis and equations in Sec. II, the entropy production is examined in the phonon-electron energy conversion systems, i.e., the hot-phonon relaxation system and the barrier energy conversion discussed in Ref. 8. The conduction electrons in  $\Gamma$ -valley in GaAs are considered for their interaction and transport, and with the parabolic band approximation, the electron density of states  $D_e$  (unit:  $\text{m}^{-3} \text{J}^{-1}$ )<sup>17</sup> is

$$D_e(E_{e,k}) = \frac{2^{1/2} m_{e,e}^{3/2} E_{e,k}^{1/2}}{\pi^2 \hbar^3}. \quad (32)$$

#### A. Hot phonon relaxation by $e-p$ and $p-p$ interactions

Hot phonons (in LO mode) in GaAs are decayed by the  $e-p$  as well as the  $p-p$  interactions, and the hot phonon relaxation process is determined by these interaction kinetics and the population distributions of the electron and phonon modes.

The primitive cell of GaAs has six phonon modes, i.e., three acoustic and three optical modes, and the LO phonon is the highest-energy phonon mode near the  $\Gamma$  point. Phonon population distribution ( $dn_p/dE_p$ , phonon population in unit volume and unit energy range) is found using the density of states ( $D_p$ ) and the occupancy ( $f_p$ ), that is,  $dn_p/dE_p = D_p f_p$ . As in the previous sections, two phonon subsystems, namely, LO phonon and other phonon modes,

are considered and, in this analysis, the phonons with energy less than  $E_{p,LO,m}$  are regarded as the other phonon modes ( $p, A$ ), when  $\int_0^{E_{p,LO,m}} D_p dE_p = 5/V_{prim}$  ( $E_{p,LO,m} = 32.7$  meV) using  $D_p$  (unit:  $\text{m}^{-3} \text{J}^{-1}$ ) from Ref. 22 and  $V_{prim}$  is the volume of the primitive cell. With a parabolic band structure, the electron density of states ( $D_e$ ) is calculated through Eq. (32). The equilibrium population distribution ( $dn_e^0/dE_e$ ) is obtained using this  $D_e$  and the equilibrium electron occupancy ( $f_e^0$ ).

Initially, the electron and phonon temperatures (except for the LO phonon mode) are set to 300 K ( $T_e = T_{p,A} = 300$  K), and for a hot phonon system, we assume that LO mode phonons are singly excited ( $f_{p,LO} = 1.0$ ), thus the LO phonon temperature is  $T_{p,LO} = 600$  K. The Fermi level ( $E_F$ ) and the total electron number density ( $n_e$ ) are assumed to be constant during the relaxation, and here the Fermi level is 0.05 eV below the conduction band edge ( $E_c - E_F = 0.05$  eV). The interaction between electrons and the LO phonons and also the LO phonon up- and downconversion are included, and the interaction rates ( $e \leftrightarrow p, LO$  and  $p, LO \leftrightarrow p, A$ ) are calculated using the Fermi golden rule as suggested in Refs. 8, 16, and 19. (Interaction time constants in GaAs range from 0.1 to 0.5 ps for  $e \leftrightarrow p, LO$  and from 2 to 10 ps for  $p, LO \leftrightarrow p, A$ .) Based on the interaction kinetics, the evolutions of the population distribution and entropy in electron and phonon systems during the hot phonon relaxation process are examined. Phonon and electron population distributions are updated at every time step ( $\Delta t_s = 10$  fs), and their entropies are calculated using Eqs. (1) and (2).

Figure 4 shows the electron and phonon energy distributions after elapsed times of 0, 1, and 10 ps after the hot phonon relaxation begins. Due to the faster  $e-p$  interaction rate compared to the  $p-p$ , the electron is first excited and relaxed to equilibrium during the hot-phonon relaxation process, so within 1 ps it has large population at high  $E_e$  (desirable for the barrier transition). This demonstrates that the hot

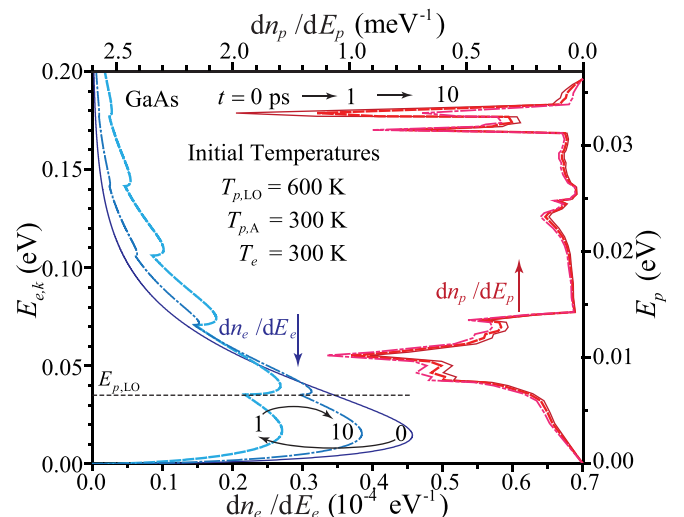


FIG. 4. The hot phonon relaxation shown for three elapsed times (0, 1, and 10 ps). The  $x$  axes represent the populated electron (lower) or phonon (upper) density, initially at the temperatures shown,  $dn_i^0/dE_i = D_i f_i^0(T_i)$  ( $D_i$  is density of states and  $f_i^0$  is occupancy function,  $i = e$  or  $p$ ). Since the  $p-p$  relaxation competes with  $e-p$ , the high energy electrons are most populated after about 1 ps.

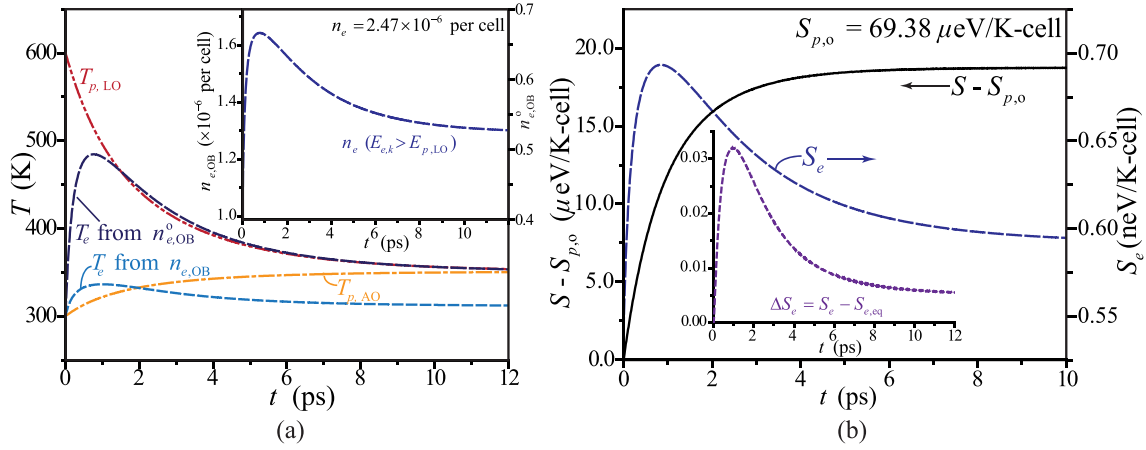


FIG. 5. (a) Time evolution of the temperatures. Inset shows the evolution of the number density ( $n_{e,OB}$ ) and fraction ( $n_{e,OB}^0$ ) of electrons with  $E_{e,k} > E_{p,LO}$ , showing the number density peaking near 1 ps.  $T_e$  first increases and then decreases, while  $T_{p,LO}$  decreases and  $T_{p,A}$  increases monotonically. For nonequilibrium electrons, the temperatures at which equilibrium distribution has the same fraction ( $n_{e,OB}^0$ ) and density ( $n_{e,OB}$ ) and density ( $n_{e,OB}$ ) of electrons over  $E_{p,LO}$  (which can be used as a barrier height) are used. (b) Entropy ( $S$ ) evolution of hot-phonon relaxation processes ( $S_{p,o}$  is the initial phonon entropy). The system entropy  $S$  ( $= S_e + S_p$ ) increases with time.

phonons should be used quickly and close to their emission site, so the barrier structure should be located near the source for in-situ phonon recycling.

When a barrier height ( $\phi_b$ ) close to  $E_{p,LO}$  is considered, the number density ( $n_{e,OB}$ ) and fraction ( $n_{e,OB}^0$ ) of electrons with  $E_{e,k} > \phi_b$  vary with respect to time as shown in the inset of Fig. 5(a). This number density or fraction peaks close to 1 ps, and this also manifests the optimum time for the barrier transition. During the relaxation, the electron distribution is not in equilibrium, so no single temperature exists. Then, multiple effective temperatures at which equilibrium distribution has the same fraction ( $n_{e,OB}^0$ ) and density ( $n_{e,OB}$ ) of electrons over  $E_{p,LO}$ , are possible. As Fig. 5(a) shows,  $T_e$  first increases and then decreases, while  $T_{p,LO}$  decreases and  $T_{p,A}$  increases monotonically. The electron and phonon entropies ( $S_e$  and  $S_p$ ) evaluated using the population distributions indicate a continuous increase in the total (system) entropy ( $S_e + S_p$ ), as shown in Fig. 5(b), even though the electron entropy decreases after 1 ps and the total entropy production rate is reduced. The results of the analysis show that in spite of the faster hot-phonon relaxation by the electrons, the hot, the optical phonon energy is also converted to lower, acoustic phonon energy, and the phonon system entropy production is larger than that for the electron system. This is because of the large population of the phonons (five order-of-magnitude larger than electrons).

## B. Barrier transition conversion

The energy and entropy in a potential barrier for converting phonon energy to electric potential are now examined to find the theoretical potential gain and conversion efficiency. As in Ref. 8, the GaAs-based barrier system is considered for a steady state, 1-D transport ( $z$ -direction), and the flux vectors for the entropy, energy, and particle number density are described in Fig. 6. Constant phonon temperature ( $T_p$ ) is assumed [it varies very little in small dimension with a much larger phonon density than electron, as demonstrated in Ref. 8]. The injected electron distribution (at the left

boundary,  $dn_{e,L}/dE_e$ ) is under equilibrium, and the electron temperature ( $T_{e,L}$ ), number density ( $n_{e,L}$ ), and the Fermi energy ( $E_{F,L}$ ) are related to one another. In this analysis,  $T_{e,L} = 300$  K and  $n_{e,L} = 10^{16}$   $\text{cm}^{-3}$  are used, then  $E_{F,L}$  is 0.094 eV below the conduction band edge ( $E_c$ ).

The barrier (with a height  $\phi_b$ ) is located just before the right boundary. Due to the barrier transition, the exiting electron distribution ( $dn_{e,R}/dE_e$ ) deviates from the equilibrium and the electron density at the right boundary is expected to be smaller than that at the left ( $n_{e,R} < n_{e,L}$ ). Thus, to maintain a current density, the drift velocity at right boundary should be larger ( $u_{e,d,R} > u_{e,d,L}$ ), and the electrochemical potential gain is defined as the difference between the Fermi levels at the right and the left boundaries ( $\Delta\phi_e = E_{F,R} - E_{F,L}$ ).

Under steady-state electron transport, the particle number and the energy conservation are given by Eqs. (22) and (24), and Eq. (31) should be satisfied for the second law of thermodynamics. For this barrier system, the energy

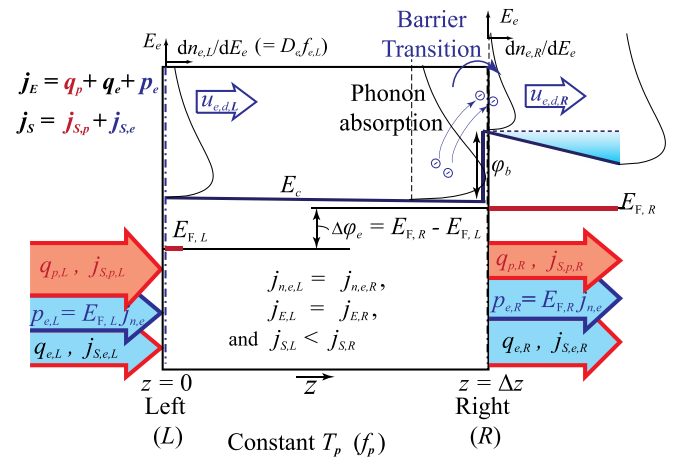


FIG. 6. The energy and entropy flux around the barrier structure under steady state. The barrier is located just before the right boundary. Phonon temperature is prescribed as  $T_p$ , and the injected electron distribution ( $dn_{e,L}/dE_e$ ) corresponds to equilibrium, while the exit distribution ( $dn_{e,R}/dE_e$ ) is not. With electrochemical potential gain  $\Delta\phi_e (= E_{F,R} - E_{F,L})$ , entropy is produced in the system, conserving the electron number and energy.

conversion efficiency (from the phonon energy to electric potential) is the ratio of the power gain (from potential gain) and the phonon energy absorption rate,

$$\eta_{p \rightarrow e} = \frac{\Delta p_{e,z}}{\dot{S}_{p \rightarrow e}/A_z} = \frac{\Delta \varphi_e j_{n,e,z}}{\int (q'_{e,R} - q'_{e,L}) dE_e + \Delta \varphi_e j_{n,e,z}} \quad (33)$$

With the prescribed conditions for electrons at the left boundary and phonons, the properties of electrons at the right boundary such as the population distribution and the Fermi levels should be defined. Here, the electron population distribution at the right boundary (right after a barrier transition) is estimated using the lateral momentum conservation (no momentum changes in  $x$  and  $y$  directions).<sup>23</sup> Excluding the scattering by other energy carriers at the barrier (because of the small dimension) (i.e., without  $e$ - $p$  or  $e$ - $e$  interaction at the barrier), there is only energy conversion between electron kinetic and potential.

The potential varies only in the transport direction, and the  $z$ -direction momentum ( $\kappa_z$ ) will decrease after the barrier transition. Therefore, the electrons with  $\kappa_z$  less than the barrier momentum [ $\kappa_b = (2m_{e,e}\varphi_b)^{0.5}/\hbar$ ] will be reflected, and the ones with  $\kappa_z > \kappa_b$  will lose their momentum by  $\kappa_b$ . For  $E_{e,k} \leq \varphi_b$ , no electron can have  $\kappa_z$  larger than  $\kappa_b$ , and even with larger electron kinetic energy ( $E_{e,k} > \varphi_b$ ), the electrons with smaller  $\kappa_z$  than  $\kappa_b$  are reflected.

The fraction of transmitted electron population can be obtained using a simple geometric calculation, as shown in Fig. 7(a). The electrons with  $E_{e,k}$  ranging from  $E_{e,k,1}$  to  $E_{e,k,2}$

(where  $E_{e,k,1} = E_{e,k} - 0.5\Delta E_{e,k}$ ,  $E_{e,k,2} = E_{e,k} + 0.5\Delta E_{e,k}$ , and  $\Delta E_{e,k}$  is a small energy step) are uniformly distributed in the spherical shell between  $E_{e,k,1}$  and  $E_{e,k,2}$ , and then the fraction for barrier transition is the ratio of the spherical shell volume with dark red and the volume with dark and light red in Fig. 7(a).

The barrier blocks the current of low-energy (or momentum) electrons, and this causes the low-energy electron accumulation. Therefore, a more favorable condition to phonon absorption is created, and then it also populates higher energy electrons, as described in Fig. 7(b). More phonon absorption brings a larger electron density ( $n_{e,R}$ ) and a smaller drift velocity ( $u_{e,d,R}$ ) after the barrier transition (although  $n_{e,R}$  should be smaller than  $n_{e,L}$  and  $u_{e,d,R}$  be larger than  $u_{e,d,L}$ ), and smaller drift velocity requires a smaller electric field (or potential drop by this field) after the barrier. When the potential drop by the internal field is allowed until the electron density recovers as  $n_{e,L}$  (where  $E_c - E_F$  is the same as the left), a higher electrochemical potential gain ( $\Delta\varphi_e$ ) can be expected by the larger phonon absorption (because a smaller electric potential drop is required with larger  $n_{e,R}$ ).

The barrier transmission (the fraction of the transmitted electrons) with respect to electron kinetic energy ( $E_{e,k}$ ) is calculated with a given barrier height ( $\varphi_b = 30$  meV), as shown in Fig. 7(c). As the electron energy increases, a larger number of electrons can have momentum over  $\kappa_b$ , and this results in a higher transmission. Based on this transmission, the electron population distribution at the right boundary ( $dn_{e,R}/dE_e$ ) is found assuming the distribution right before the

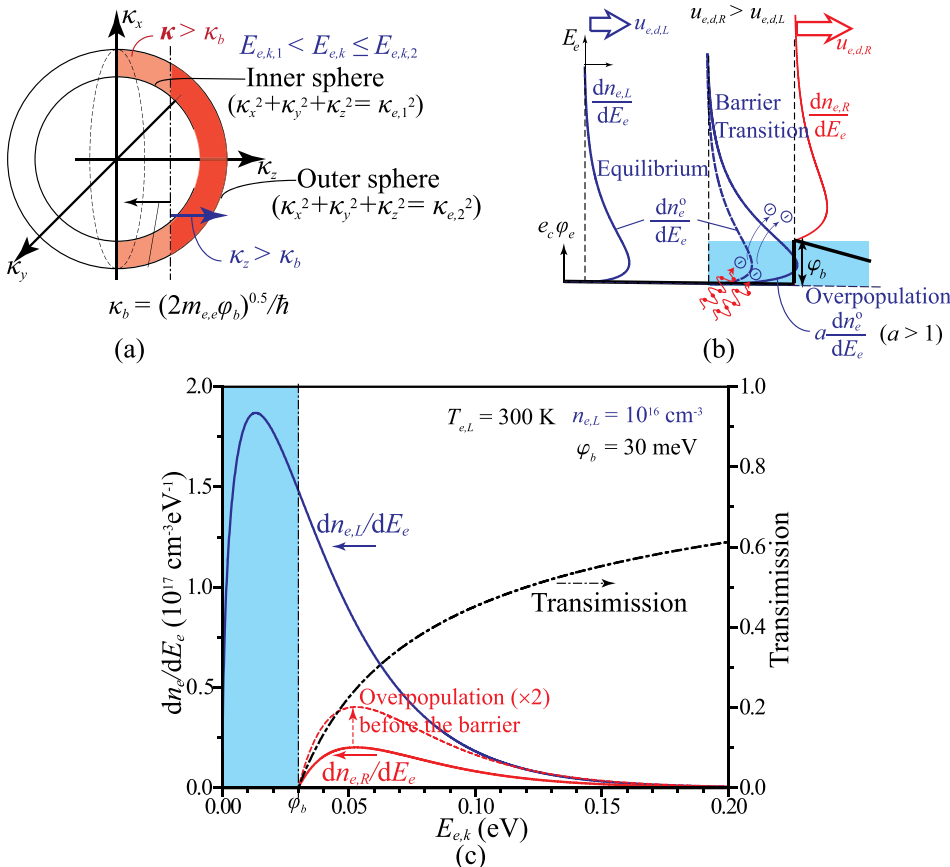


FIG. 7. (a) The fraction of transmitted electron population at energy level  $E_{e,k}$  ( $E_{e,k,1} < E_{e,k} < E_{e,k,2}$ ). With the lateral momentum conservation, electrons with larger momentum than the barrier momentum [ $\kappa_b = (2m_{e,e}\varphi_b)^{0.5}/\hbar$ ] can be transmitted, losing their  $z$ -direction momentum by  $\kappa_b$ . The fraction is the ratio of volume of the spherical shell with dark red to the volume with dark and light red. (b) Due to the barrier, low-energy electrons are more populated, and this leads to larger phonon absorption and populates higher energy electrons. Smaller electron number density after the barrier transition also causes a larger drift velocity for a constant electric current. (c) Electron population distributions at the left and right boundaries ( $dn_{e,L}/dE_e$  and  $dn_{e,R}/dE_e$ ), and the variations of barrier transmission with respect to electron kinetic energy ( $E_{e,k}$ ). Electrons at the left boundary correspond to equilibrium with  $T_{e,L} = 300$  K and  $n_{e,L} = 10^{16} \text{ cm}^{-3}$ , and  $\varphi_b$  is 30 meV. As the electron energy increases, larger number of electrons can have momentum over  $\kappa_b$ , and this results in higher transmission. Due to the overpopulation (by barrier) with phonon absorption, the electron density at right boundary can increase.

barrier. When we assume the same distribution (without phonon absorption) as on the left boundary distribution  $dn_{e,L}/dE_e$  (equilibrium with  $T_{e,L} = 300$  K and  $n_{e,L} = 10^{16}$  cm $^{-3}$ ),  $dn_{e,R}/dE_e$  is calculated as shown with the red-solid line in Fig. 7(c). With the overpopulation by barrier, a larger population of electron distribution at the right boundary is expected because of the phonon absorption.

Once the electron distributions at both boundaries are found, the theoretical range of the electrochemical potential gain  $\Delta\phi_e$  and the energy conversion efficiency  $\eta_{p\rightarrow e}$  are calculated using the continuity equation and the first and second laws of thermodynamics [Eqs. (22), (24), and (31)]. In the electric current, the phonon temperature cannot be higher than electron temperature, because the energy flows from electron to phonon systems as electric potential is the source for the Joule heating. With interest in recycling the Joule heating as in the hot-phonon absorbing barrier system,<sup>8</sup> the case of the phonon temperature ( $T_p$ ) equal to  $T_{e,L}$  (as the maximum possible temperature) is considered first.

The energy and entropy fluxes are calculated through the numerical integration using the electron population distribution ( $D_{ef}$ ) and the drift velocity ( $u_{e,d,z}$ ). The drift velocity can change with  $E_e$ , but a constant  $u_{e,d,z}$  for all  $E_e$  is assumed for simplicity. From  $n_{e,R}$ , the average electron drift velocity ( $u_{e,d,R}$ ) and the Fermi level  $E_{F,R}$  (for potential gain) at the right boundary are determined. ( $u_{e,d,R}$  should be inversely proportional to  $n_{e,R}$  for a constant electric current). Varying  $n_{e,R}$  [i.e., changing the degree of overpopulation ( $a > 1$ ) behind the barrier, as in Fig. 7(b)], the net entropy flux  $\Delta j_{S,z}$  and potential gain  $\Delta\phi_e$  are calculated, and using Eq. (33), the energy conversion efficiency (for phonon energy conversion to electrochemical potential)  $\eta_{p\rightarrow e}$  is also found.

Figure 8 demonstrates that  $\eta_{p\rightarrow e}$  increases and  $\Delta j_{S,z}$  decreases as  $\Delta\phi_e$  increases (by larger  $n_{e,R}$  from more phonon absorption). For the 1-D, steady-state transport system,  $\Delta j_{S,z}$  represents the entropy production rate per unit area in the control volume, and this rate should be positive. Therefore,

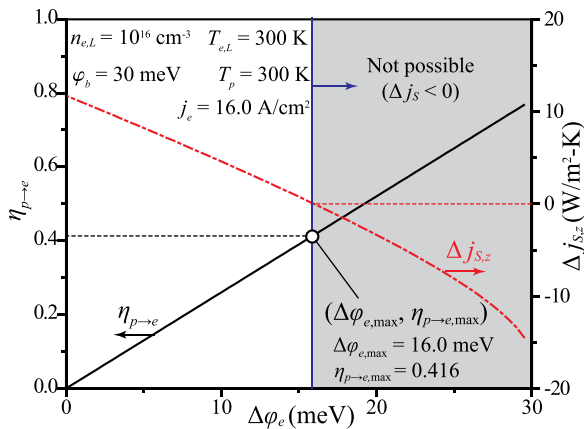


FIG. 8. Variations of energy conversion efficiency ( $\eta_{p\rightarrow e}$ ) and the net entropy flux ( $\Delta j_{S,z}$ ) with respect to the potential gain ( $\Delta\phi_e$ ). Here  $\Delta j_{S,z}$  represents the entropy production rate per unit area in the 1-D transport system. As  $\Delta\phi_e$  increases,  $\eta_{p\rightarrow e}$  increases and the entropy production rate decreases. The maximum efficiency ( $\eta_{p\rightarrow e,max}$ ) and potential gain ( $\Delta\phi_{e,max}$ ) are found with  $\Delta j_{S,z} = 0$ .

the maximum efficiency ( $\eta_{p\rightarrow e,max}$ ) and the potential gain ( $\Delta\phi_{e,max}$ ) are found when  $\Delta j_{S,z} = 0$ . When  $T_p = T_e = 300$  K and  $\phi_b = 30$  meV, the predicted theoretical maximum efficiency is 41.6% with 16.0 meV as the maximum potential gain.

For variable potential barrier heights ( $\phi_b$ ), the values of  $\Delta\phi_{e,max}$  and  $\eta_{p\rightarrow e,max}$  are calculated under zero entropy production ( $\Delta j_{S,z} = 0$ ). As Fig. 9 shows,  $\Delta\phi_{e,max}$  increases with  $\phi_b$ , while  $\eta_{p\rightarrow e,max}$  has a maximum at  $\phi_b = 12$  meV. In this analysis, the overpopulation before the barrier is simply assumed to be proportional to that of equilibrium, but with dominant LO phonon interaction, the population distribution is stratified with a period of  $E_{p,LO}$  as shown in Fig. 4, and this increases the maximum efficiency barrier height.

Assuming an external phonon source, this barrier system is analyzed for variable phonon temperature ( $T_p$ ), including  $T_p > T_{e,L}$ . Also, assuming that the LO phonon interaction is only available between the electron and the phonon systems ( $e$ - $p$ , LO interactions dominant in GaAs), the nonequilibrium among phonon modes (LO and A) can be considered. A high  $T_{p,LO}$  leads to large  $\Delta\phi_{e,max}$  and  $\eta_{p\rightarrow e,max}$ , as shown in Figs. 10(a) and 10(b). With hot LO phonons ( $T_{p,LO} > T_{p,A}$ ), the inclusion of the  $p$ - $p$  interactions (LO phonon downconversion) decreases  $\Delta\phi_{e,max}$  and  $\eta_{p\rightarrow e,max}$ .

As this analysis shows (and is expected), the theoretical maximum efficiency is higher than the results of the MC simulations [19% for  $T_e = T_{p,A} = T_{p,LO} = 300$  K (Ref. 8)]. Because the electron-phonon interactions are present and any such spontaneous interaction produces entropy, the entropy production in the energy conversion system should be larger than zero. Therefore, the efficiency  $\eta_{p\rightarrow e}$  is smaller than  $\eta_{p\rightarrow e,max}$ . In addition, the inclusion of more interaction mechanisms, such as the  $p$ - $p$  and  $e$ - $e$ , will further decrease the efficiency. The entropy production, which affects the conversion efficiency, depends on the barrier parameters and the interaction kinetics, so the barrier structure should be optimized for minimum entropy production and maximum efficiency. Due to the assumptions made here (e.g., symmetric distribution in  $\kappa$ -space), the results do not depend on electron drift velocity ( $u_{e,d,z}$ ), but in a practical system,  $u_{e,d,z}$  is

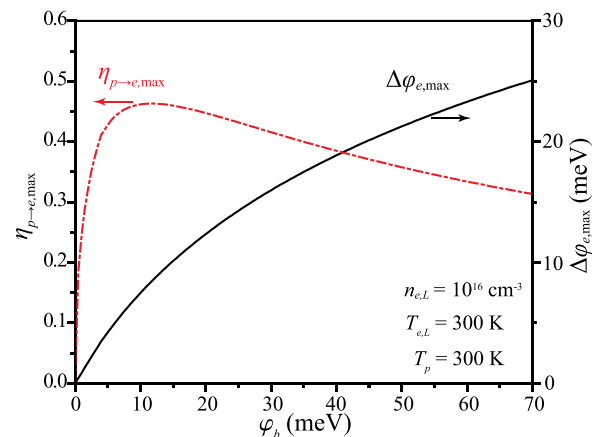


FIG. 9. Variations of the maximum potential gain ( $\Delta\phi_{e,max}$ ) and the maximum energy conversion efficiency ( $\eta_{p\rightarrow e,max}$ ) with respect to the potential barrier height ( $\phi_b$ ).  $\Delta\phi_{e,max}$  increases with  $\phi_b$ , while  $\eta_{p\rightarrow e,max}$  reaches a maximum at  $\phi_b = 12$  meV.

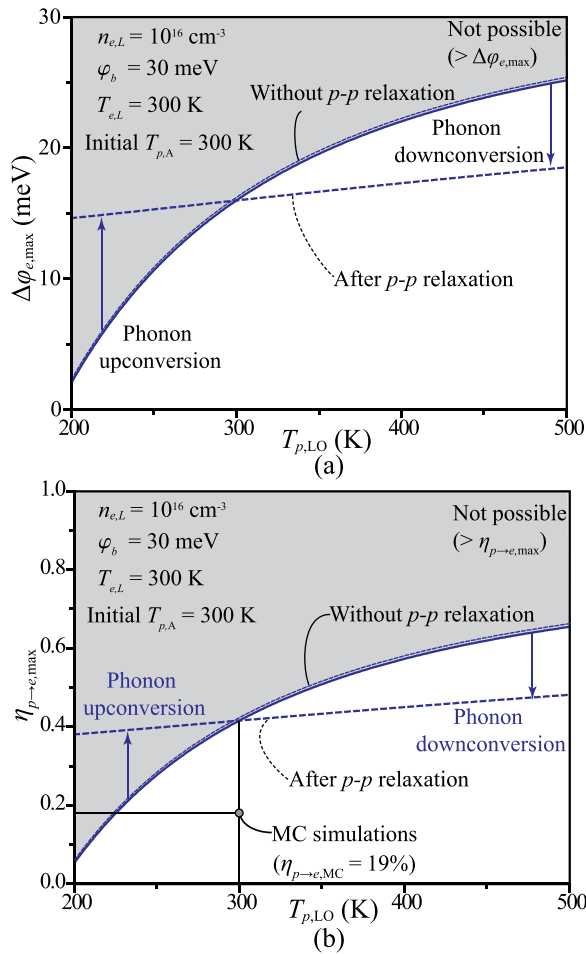


FIG. 10. Effects of the LO phonon temperature ( $T_{p,LO}$ ) on (a) the maximum potential gain ( $\Delta\phi_{e,\max}$ ) and (b) the maximum conversion efficiency ( $\eta_{p \rightarrow e, \max}$ ), when LO phonon interactions dominate. The high phonon temperature leads to large  $\Delta\phi_{e,\max}$  and high  $\eta_{p \rightarrow e, \max}$ . With an overpopulated LO phonons ( $T_{p,LO} > T_{p,A}$ ), the inclusion of the  $p-p$  interactions<sup>8</sup> reduces  $\eta_{p \rightarrow e, \max}$  and  $\Delta\phi_{e,\max}$ . The efficiency from the MC simulations<sup>8</sup> is lower than this theoretical upper limit  $\eta_{p \rightarrow e, \max}$ .

related to the electron distribution and the electric field (or potential), and these affect the conversion efficiency  $\eta_{p \rightarrow e}$ .

#### IV. CONCLUSIONS

By addressing the statistical entropy and nonequilibrium populations of the phonon and electron systems with phonon-phonon and electron-phonon interactions, we derived expressions for the overall entropy production in phonon energy conversion to electric potential. We noted that the spontaneous interaction will increase the system entropy, and the energy carrier temperatures indicate the direction of energy flow. Since optical phonons are emitted in many circuits and devices, they can be recycled. The hot-

phonon relaxation processes indicate that these hot phonons should be used quickly and close to their emission site for higher conversion efficiency, so the barrier structure should be located near the source.

In the entropy analysis and its applications, we used the first and the second laws of thermodynamics (i.e., energy conservation and entropy production), and predicted the maximum efficiency under the minimum entropy production condition. For the GaAs:Al heterobarrier structure introduced and discussed in Ref. 8, the spontaneous phonon absorption is achieved through lower electron temperatures created by converting electron kinetics to potential in a barrier structure. We find the upper limit of the phonon-electron potential conversion efficiency using this entropy analysis. As expected, the non-ideal, irreversible MC simulation results for efficiency are lower than this theoretical upper limit.

#### ACKNOWLEDGMENTS

The support by NSF Program on Thermal Transport and Processes, through Award 0966229, is greatly appreciated.

- <sup>1</sup>M. W. Zemansky and R. Dittman, *Heat and Thermodynamics* (McGrawHill, New York, 1997).
- <sup>2</sup>J. Kestin, *A Course in Thermodynamics* (Blaisdell, Waltham, 1966).
- <sup>3</sup>G. Maugin, *The Thermomechanics of Nonlinear Irreversible Processes* (World Scientific, Singapore, 1999).
- <sup>4</sup>L. Landau, *J. Phys. (Moscow)* **10**, 503 (1946).
- <sup>5</sup>X. L. Ruan, S. C. Rand, and M. Kaviany, *Phys. Rev. B* **75**, 214304 (2007).
- <sup>6</sup>R. C. Tolman and P. Fine, *Rev. Mod. Phys.* **20**, 51 (1948).
- <sup>7</sup>C. Goupil, W. Seifert, K. Zabrocki, E. Müller, and G. J. Snyder, *Entropy* **13**, 1481 (2011).
- <sup>8</sup>S. Shin, C. Melnick, and M. Kaviany, *Phys. Rev. B* **87**, 075317 (2013).
- <sup>9</sup>L. Boltzmann, *Lecture Notes on Gas Theory, Translated from the German Editions (Part 1; 1896, and Part 2; 1898)* (Dover, New York, 1964).
- <sup>10</sup>O. Eriksson, J. M. Wills, and D. Wallace, *Phys. Rev. B* **46**, 5221 (1992).
- <sup>11</sup>P. T. Landsberg and G. Tonge, *J. Appl. Phys.* **51**, R1 (1980).
- <sup>12</sup>P. D. Bogdanoff, B. Fultz, J. L. Robertson, and L. Crow, *Phys. Rev. B* **65**, 014303 (2001).
- <sup>13</sup>C. Kittel, *Thermal Physics* (W. H. Freeman and Company, New York, 1980).
- <sup>14</sup>K. Kim, K. Hess, and F. Capasso, *Appl. Phys. Lett.* **52**, 1167 (1988).
- <sup>15</sup>K. Wang, J. Simon, N. Goel, and D. Jena, *Appl. Phys. Lett.* **88**, 022103 (2006).
- <sup>16</sup>G. Srivastava, *The Physics of Phonons* (Adam Hilger, Bristol, 1995).
- <sup>17</sup>M. Kaviany, *Heat Transfer Physics* (Cambridge University Press, Cambridge, 2008).
- <sup>18</sup>E. Bringuier, *Phys. Rev. E* **61**, 6351 (2000).
- <sup>19</sup>M. Lundstrom, *Fundamentals of Carrier Transport* (Cambridge University Press, Cambridge, 2000).
- <sup>20</sup>J. S. Blakemore, *J. Appl. Phys.* **53**, R123 (1982).
- <sup>21</sup>M. Shur, *GaAs Devices and Circuits* (Springer, New York, 1987).
- <sup>22</sup>P. Giannozzi, S. de Gironcoli, P. Pavone, and S. Baroni, *Phys. Rev. B* **43**, 7231 (1991).
- <sup>23</sup>R. Kim, C. Jeong, and M. Lundstrom, *J. Appl. Phys.* **107**, 054502 (2010).